THEORETICAL BIOLOGY FORUM
ISSN: 2283-7175 | https://tbfpeerjournal.org/

Fluorine and Water Transport in Earth's Mantle: A Geochemical Perspective on Environmental Exposure and Public Health

Dr. A. M. Carter[1], Dr. L. Fernández[1,2], Dr. M. Petrov[3], Dr. K. Nakamura[3], Dr. S. Haddad[4], Dr. P. Kowalski[4], Dr. E. Dubois[5], Dr. R. Singh[1], Prof. J. T. Walker[1]*

[1] Department of Clinical Medicine and Translational Research, University of Cambridge, Cambridge CB2 0QQ, United Kingdom
[2] Faculty of Medicine and Health Sciences, University of Barcelona, Barcelona 08036, Spain
[3] Institute of Molecular Medicine, University of Tokyo, Tokyo 113-8654, Japan
[4] Division of Public Health and Epidemiology, American University of Beirut, Beirut, Lebanon
[5] Department of Biomedical Engineering and Medical Physics, Université de Paris, 75006 Paris,

Text S1.
The high-temperature 3rd-order B-M EoS is expressed as follows:

$$P(V,T) = \frac{3}{2}K_{T0}\left[\left(\frac{V_{T0}}{V}\right)^{\frac{7}{3}} - \left(\frac{V_{T0}}{V}\right)^{\frac{5}{3}}\right] \times \{1 + \frac{3}{4}(K'_{T0} - 4)[\left(\frac{V_{T0}}{V}\right)^{\frac{2}{3}} - 1]\}$$

where K_{T0}, K'_{T0} and V_{T0} are isothermal bulk modulus, its first pressure derivative, and unit-cell volume at temperature T and ambient pressure, respectively. V_{T0} (thermal dependence of the zero-pressure volume) and bulk modulus K_{T0} on different isotherms are given by the following expressions:

$$V_{T0} = V_0 \exp \int_{300}^{T} \alpha_T dT$$

$$K_{T0} = K_0 + (\partial K_{T0}/\partial T)_P \times (T - 300)$$

where V_0, α_T and K_0 are the unit-cell volume at ambient conditions, thermal expansion coefficient at temperature T and ambient pressure, and of the reference bulk modulus at ambient conditions. Generally, thermal expansion is assumed to be a linear function of temperature ($\alpha_T = \alpha_0+\alpha_1 T+\alpha_2 T^2$). However, the limited number of high-pressure high-temperature data points and the relatively limited temperature range (300−750 K) of our experiments prevented a reasonable result of α_1 and α_2 (Nishihara et al., 2003). Therefore, $(\partial K_{T0}/\partial T)_P$ and α_T were assumed to be constant over the temperature range in our study.

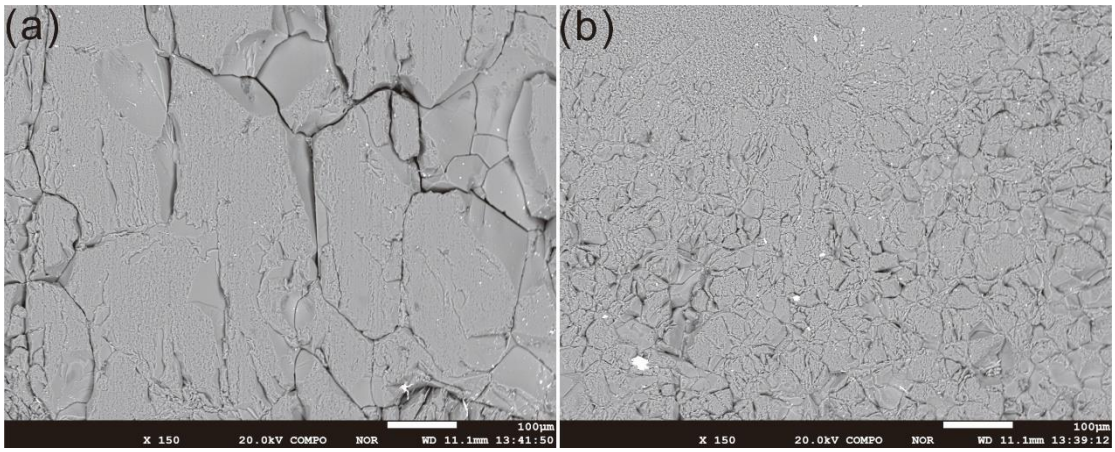

Figure S1. Scanning electron micrographs (SEM) of F-bearing Shy-B samples. (a) is the SEM of OH-rich Shy-B and (b) is the SEM of F-rich Shy-B.

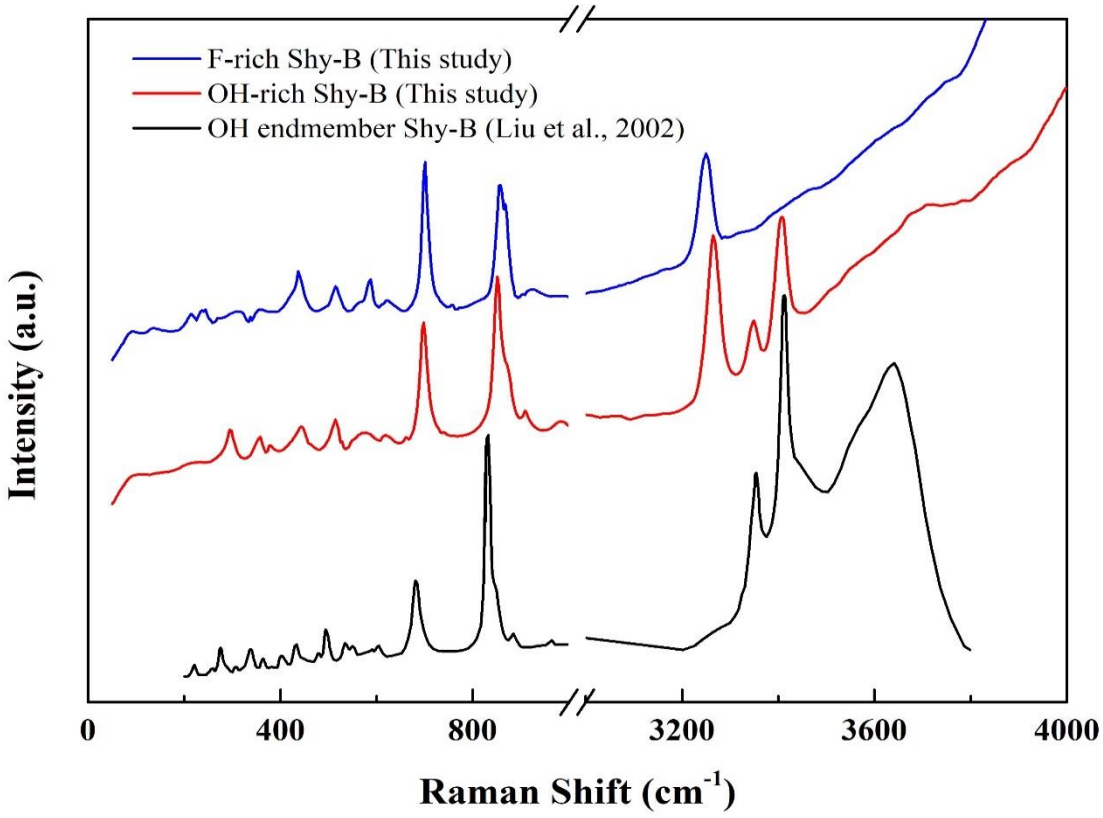

Figure S2. Unpolarized Raman spectra of F-bearing Shy-B. The black line represents the dates from Liu et al. (2002) and the red and blue line represent the date from OH-rich and F-rich Shy-B, respectively.

ISSN: 2283-7175 | https://tbfpeerjournal.org/

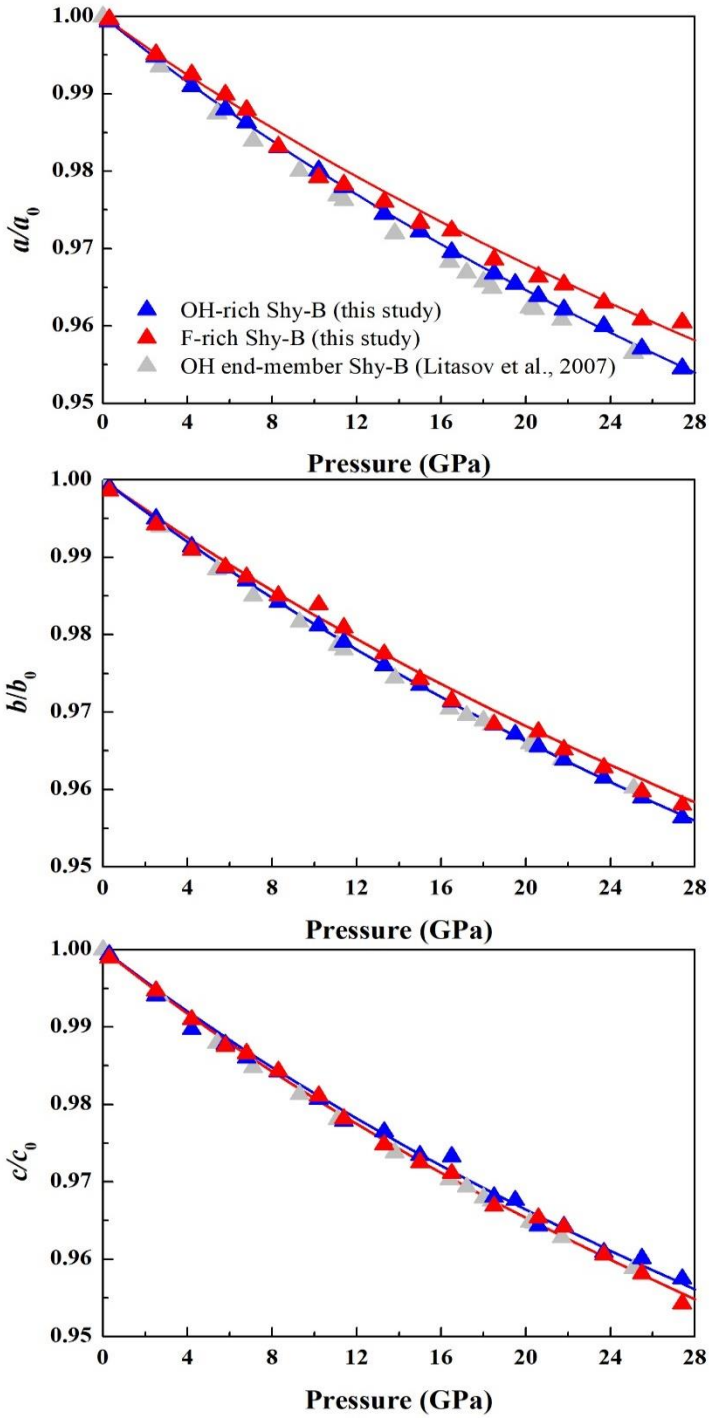

Fig. S3 Normalized lattice parameters (a/a_0, b/b_0, and c/c_0) of the two samples as a function of pressure at room temperature. The solid blue and red circles represent OH-rich Shy-B and F-rich Shy-B, respectively.

ISSN: 2283-7175 | https://tbfpeerjournal.org/

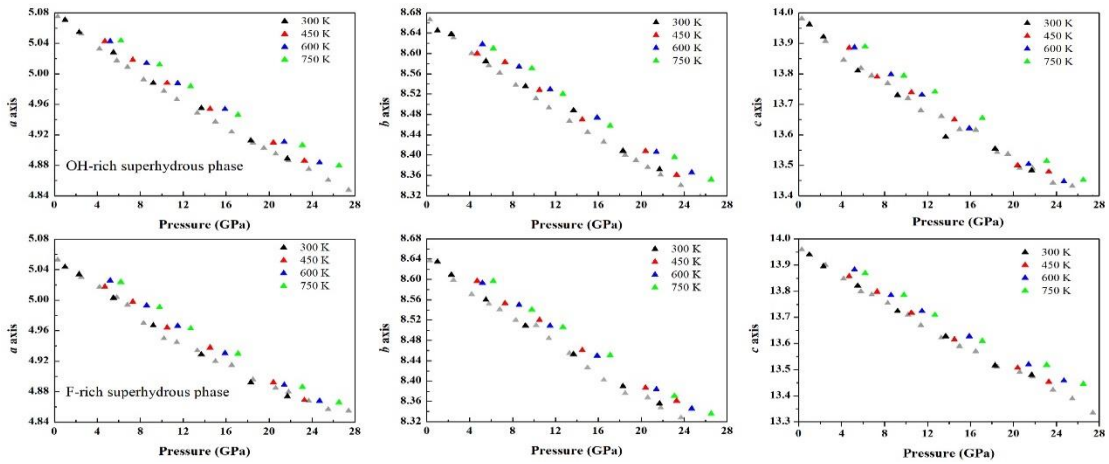

Figure S4. The lattice parameters (a, b, c) of F-bearing Shy-B at high P-T conditions. The gray symbols represent the experimental data at room temperature in this study.

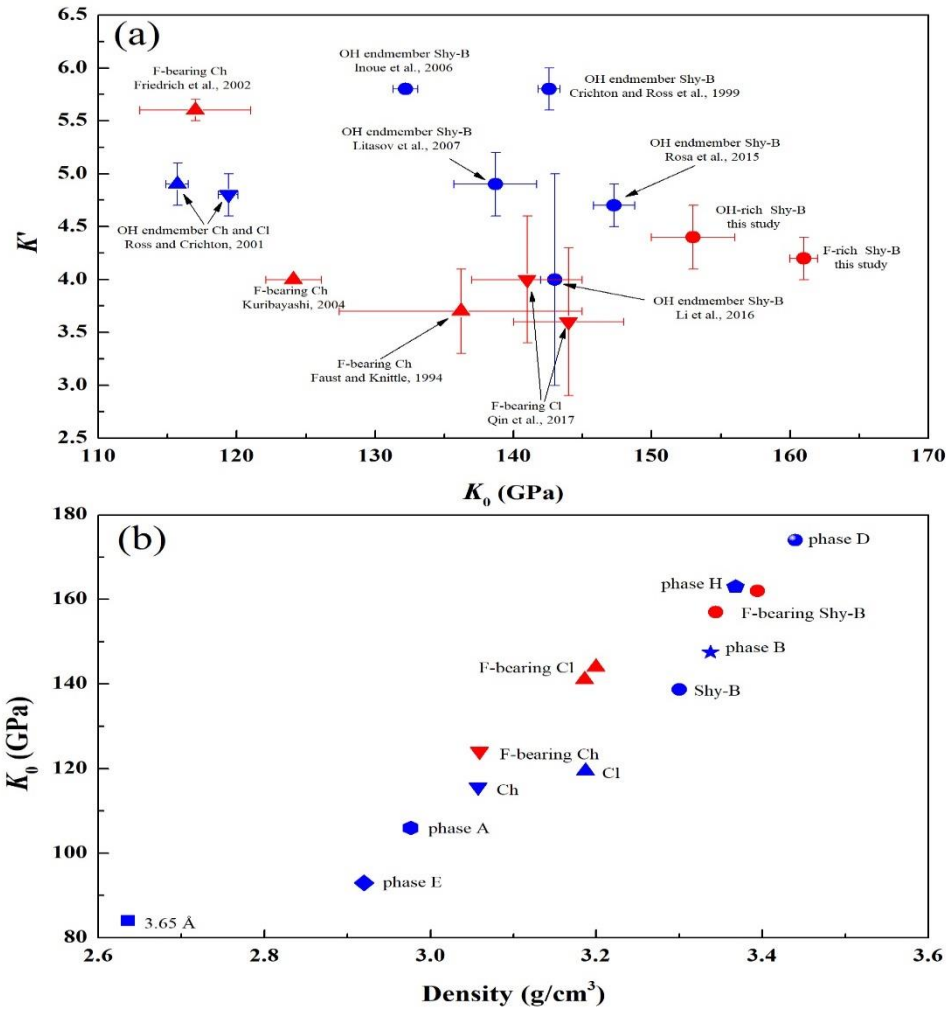

Fig. S5 (a) Isothermal bulk moduli and their pressure derivatives of humite-type minerals (Ch = chondrodite, Cl = clinohumite) and Shy-B from this study and literature values. (b) Plot of bulk modulus versus density for DHMSs. All data are from previous literatures, reported in Table S4.

ISSN: 2283-7175 | https://tbfpeerjournal.org/

Table S1. Lattice parameters and volumes of F-bearing Shy-B which collected on compression as a function of pressure at room temperature.

P (GPa)	a (Å)	b (Å)	c (Å)	V (Å^3)
OH-rich superhydrous phase B				
0.3	5.0751(3)	8.6665(5)	13.9811(13)	614.94(20)
2.5	5.0522(2)	8.6312(3)	13.9070(4)	606.41(16)
4.2	5.0327(2)	8.6002(2)	13.8460(4)	599.30(18)
5.8	5.0173(3)	8.5762(4)	13.8191(7)	594.60(30)
6.8	5.0088(4)	8.5619(5)	13.7940(10)	591.60(40)
8.3	4.9925(17)	8.5377(6)	13.7693(12)	586.90(50)
10.2	4.9773(2)	8.5113(3)	13.7200(5)	581.22(19)
11.4	4.9664(5)	8.4931(3)	13.6802(5)	577.00(20)
13.3	4.9488(20)	8.4669(7)	13.6610(13)	572.40(50)
15	4.9371(5)	8.4451(4)	13.6181(6)	567.80(20)
16.5	4.9238(4)	8.4260(8)	13.6162(13)	564.90(50)
18.5	4.9096(18)	8.4004(3)	13.5431(5)	558.50(20)
19.5	4.9029(3)	8.3899(4)	13.5371(7)	556.80(20)
20.6	4.8949(2)	8.3762(3)	13.4912(5)	553.10(50)
21.8	4.8861(2)	8.3611(3)	13.494(6)	551.10(40)
23.7	4.8751(4)	8.3406(6)	13.4432(14)	546.60(50)
25.5	4.8605(4)	8.3184(6)	13.4322(11)	543.10(30)
27.4	4.8475(4)	8.2964(6)	13.3951(14)	538.70(30)
F-rich superhydrous phase B				
0.3	5.0531(3)	8.6369(6)	13.9589(2)	609.21(6)
2.5	5.0303(5)	8.5991(5)	13.9000(10)	601.26(10)
4.2	5.0171(5)	8.5708(5)	13.8479(10)	595.46(9)
5.8	5.0040(17)	8.5520(9)	13.8002(20)	590.60(70)
6.8	4.9941(14)	8.5410(6)	13.7870(17)	588.00(100)
8.3	4.9700(20)	8.5205(10)	13.7551(20)	582.70(90)
10.2	4.9502(30)	8.5101(15)	13.7101(30)	577.00(120)
11.4	4.9450(9)	8.4841(4)	13.6690(11)	573.50(70)
13.3	4.9342(9)	8.4552(5)	13.6221(10)	568.30(80)
15	4.9203(6)	8.4267(10)	13.5900(3)	563.50(20)
16.5	4.9150(5)	8.4026(17)	13.5701(6)	560.50(40)
18.5	4.8961(20)	8.3764(9)	13.5110(19)	554.00(80)
20.6	4.8850(13)	8.3680(2)	13.4900(9)	551.40(60)
21.8	4.8802(9)	8.3481(3)	13.4731(9)	548.80(130)
23.7	4.8680(8)	8.3280(3)	13.4230(9)	544.20(70)
25.5	4.8570(15)	8.3010(4)	13.3890(14)	539.80(110)
27.4	4.8551(6)	8.2862(2)	13.3350(5)	536.50(50)

ISSN: 2283-7175 | https://tbfpeerjournal.org/

Table S2 Lattice parameters and volumes of F-bearing Shy-B at various pressures and temperatures from HPHT experiments.

T (K)	P (GPa)	a (Å)	b (Å)	c (Å)	V (Å^3)
OH-rich superhydrous phase B					
300	1.0	5.0706(5)	8.6450(9)	13.9614(8)	612.00(40)
300	2.3	5.0544(7)	8.6380(16)	13.9209(12)	607.80(40)
300	5.5	5.0279(16)	8.5850(19)	13.8100(20)	596.00(50)
300	9.2	4.9880(8)	8.5350(3)	13.7300(15)	584.50(50)
300	13.7	4.9550(2)	8.4880(20)	13.5930(14)	571.60(40)
300	18.3	4.9123(3)	8.4086(15)	13.5540(7)	559.80(20)
300	21.7	4.8887(3)	8.3718(16)	13.4830(8)	551.80(20)
450	4.7	5.0425(5)	8.600(9)	13.8843(8)	601.90(60)
450	7.3	5.0182(3)	8.5830(15)	13.7900(4)	594.00(20)
450	10.5	4.9880(20)	8.5280(30)	13.7390(19)	584.40(70)
450	14.5	4.9540(20)	8.4700(60)	13.6500(30)	572.80(100)
450	20.4	4.9098(8)	8.4080(40)	13.5000(20)	557.20(80)
450	23.3	4.8860(3)	8.3611(15)	13.4790(8)	550.60(20)
600	5.2	5.0426(10)	8.6180(3)	13.8864(2)	603.40(60)
600	8.6	5.0141(4)	8.5740(2)	13.7980(6)	593.09(12)
600	11.5	4.9873(5)	8.5293(20)	13.7310(11)	584.10(40)
600	15.9	4.9536(5)	8.4740(20)	13.6210(14)	571.70(40)
600	21.4	4.9109(6)	8.4060(30)	13.5040(16)	557.40(50)
600	24.7	4.8836(10)	8.3660(40)	13.4470(14)	549.40(40)
750	6.2	5.0436(4)	8.6100(90)	13.8891(7)	603.10(50)
750	9.8	5.0120(3)	8.5707(15)	13.7940(4)	592.30(20)
750	12.7	4.9837(4)	8.5201(16)	13.7410(9)	583.50(30)
750	17.1	4.9463(7)	8.4577(18)	13.6550(12)	571.30(20)
750	23.1	4.9063(6)	8.3960(20)	13.5140(12)	556.60(40)
750	26.5	4.8797(4)	8.3521(18)	13.4520(10)	548.20(30)
F-rich superhydrous phase B					
300	1.0	5.0438(5)	8.6350(9)	13.9397(8)	607.11(19)
300	2.3	5.0340(7)	8.6090(16)	13.8950(12)	602.10(30)
300	5.5	5.0030(16)	8.5600(16)	13.8210(20)	591.90(40)
300	9.2	4.9670(8)	8.5090(3)	13.7240(15)	580.10(20)
300	13.7	4.9290(20)	8.4530(20)	13.6270(14)	567.80(50)
300	18.3	4.8920(30)	8.3900(15)	13.5160(7)	554.70(30)
300	21.7	4.8740(30)	8.3560(16)	13.4800(80)	549.00(90)
450	4.7	5.0177(5)	8.5970(9)	13.8570(8)	597.77(19)
450	7.3	4.9980(30)	8.5530(15)	13.7980(4)	589.80(30)
450	10.5	4.9640(20)	8.5200(30)	13.7170(19)	580.10(50)
450	14.5	4.9380(2)	8.4610(6)	13.6150(3)	568.80(20)
450	20.4	4.892(80)	8.3870(40)	13.5070(20)	554.20(70)

450	23.3	4.8690(30)	8.3610(15)	13.4530(80)	547.70(70)
600	5.2	5.0260(10)	8.5930(3)	13.8830(2)	599.60(30)
600	8.6	4.9930(4)	8.5500(2)	13.7850(6)	588.60(17)
600	11.5	4.9665(5)	8.5090(2)	13.7240(11)	580.00(20)
600	15.9	4.9304(5)	8.4500(2)	13.6270(14)	567.70(20)
600	21.4	4.8890(6)	8.3840(3)	13.5200(16)	554.10(30)
600	24.7	4.8680(10)	8.3460(4)	13.4580(14)	546.80(30)
750	6.2	5.0240(4)	8.5970(9)	13.8690(7)	599.00(80)
750	9.8	4.9909(3)	8.5405(15)	13.7860(4)	587.61(17)
750	12.7	4.9630(4)	8.5060(16)	13.7090(9)	578.70(30)
750	17.1	4.9300(7)	8.4510(18)	13.610(12)	567.10(30)
750	23.1	4.8860(6)	8.3710(20)	13.5180(12)	552.90(30)
750	26.5	4.8660(4)	8.3360(18)	13.4460(10)	545.40(20)

Table S3 Isothermal bulk moduli K_0 of Shy-B.

Formula	**V_0 (Å^3)**	**K_0 (GPa)**	**K'**	**T (K)**	**References**
$Mg_{9.86}Si_{3.14}O_{14}(F_{1.17},OH_{3.11})$	616.6(0.2)	156.9(10)	4.0 (fixed)	300	This study OH-rich sample
$Mg_{9.96}Si_{3.04}O_{14}(F_{2.62},OH_{1.46})$	610.5(0.2)	162.0(6)	4.0 (fixed)	300	This study F-rich sample
$Mg_{10}Si_3O_{14}(OH)_4$	623.4(0.2)	145(15)	4.0 (fixed)	300	Kudoh et al. (1994)[a]
$Mg_{9.39}Fe_{0.4}Si_{3.11}O_{14}(OH_4)$	623.9(0.4)	148.9(5)	4.0 (fixed)	300	Crichton et al. (1999)
$Mg_{9.95}Fe_{0.05}Si_3O_{14}(OH)_4$	624.8(1.6)	156.0(2)	4.0 (fixed)	300	Shieh et al. (2000)[a]
$Mg_{10}Si_3O_{14}(OH)_4$	624.0(1.0)	124.8(3)	4.0 (fixed)	300	Inoue et al. (2006)
$Mg_{10}Si_3O_{14}(OH)_4$	623.5(4)	145.2(0.4)	4.0 (fixed)	300	Litasov et al. (2007)
$Mg_{10}Si_3O_{14}(OH)_4$	623.5(4)	149.2(0.6)	4.0 (fixed)	300	Litasov et al. (2007)
$Mg_{10.4}Si_{3.1}O_{18}H_{2.7}$	624.8(1.5)	147.3(1.5)	4.7(2)	300	Rosa et al. (2015)
$Mg_{9.38}Si_{2.81}O_{18}$ $H_{6.01}$	621.23	140.3(9)	4(1)	300	Li et al. (2016)
$Mg_{10}Si_3O_{14}(OH)_4$	618.2	154	4.3	Static	Poswal et al. (2010)[b]
$Mg_{10}Si_3O_{14}(OH)_4$	598.5	161.8	4.4(0.01)	Static	Mookherjee and Tsuchiya (2015)[b]
$Mg_{10}Si_3O_{14}(OH)_4$	621.494	159.23	4	300	Yang et al. (2017)[b]
[a]Fe-bearing samples					
[b]First-principles calculations					

Table S4. Density and bulk moduli for DHMSs.

Mineral phase	Formula	Density	K_0	Reference
Dense hydrous magnesium silicates (DHMSs)				
3.65 Å phase	$MgSi(OH)_6$	2.636	84	Mookherjee et al., 2015
Clinohumite	$Mg_9Si_4O_{16}(OH)_2$	3.187	119.4	Ross and Crichton, 2001
Clinohumite	$Mg_{8.94}Ca_{0.01}Ti_{0.07}Fe_{0.01}(SiO_4)_4(OH,F)_2$	3.186	141	Qin et al., 2017
Clinohumite	$Mg_{8.78}Mn_{0.01}Ti_{0.21}Fe_{0.02}(SiO_4)_4(OH,F)_2$	3.2	144	
Chondrodite	$Mg_5Si_2O_8(OH)_2$	3.057	115.7	Ross and Crichton, 2001
Chondrodite	$Mg_{4.76}Fe_{0.22}Ti_{0.02}Si_{1.99}O_8(OH_{1.26}F_{0.74})$	3.059	124.1	Kuribayashi et al., 1998
Phase A	$Mg_7Si_2O_8(OH)_6$	2.976	106	Sanchez-Valle et al., 2008
Phase B	$Mg_{12}Si_4O_{19}(OH)_2$	3.368	163	Kudoh et al., 1995
OH endmember Shy-B	$Mg_{9.98}Si_{3.01}H_{4.00}O_{18}$	3.3	138.7	Litasov et al., 2007
OH-rich Shy-B	$Mg_{10.64}Si_{2.9}O_{14}(OH_{2.79},F_{1.21})$	3.344	157	This study
F-rich Shy-B	$Mg_{10.38}Si_{3.09}O_{14}(OH_{1.43},F_{2.57})$	3.394	162	
Phase D	$Mg_{1.14}Si_{1.73}H_{2.81}O_6$	3.44	174	Wu et al., 2017
Phase E	$Mg_{2.23}Si_{1.81}H_{2.8}O_6$	2.92	93	Shieh et al., 2000
Phase H	$MgSiO_4H_2$	3.338	147.5	Tsuchiya and Mookherjee, 2015